31st Congress of the International Council of the Aeronautical Sciences

Belo Horizonte, Brazil; September 09-14, 2018

LATTICE BOLTZMANN HIGH-LIFT SIMULATIONS – A STEP BEYOND CLASSICAL CFD

Benedikt König , Deepali Singh , Ehab Fares
Exa GmbH, Curiestrasse 4, 70563 Stuttgart, Germany

Keywords: *LBM, JSM, stall*

Abstract

A Lattice Boltzmann CFD method is employed to highlight the impact of certain simplifications and limitations that are often encountered when simulating high-lift flows. On the example of the JAXA JSM model, the effect of reduced geometrical fidelity is considered, the unsteady behaviour of the flow described, and the difficulties of classical CFD in predicting the wake and vortex interactions correctly is shown. It is demonstrated how these often encountered limitations can be resolved by using a Lattice Boltzmann method based approach.

1 Introduction

High-lift flow is often dominated by large and thereby unsteady flow separations as well as by a significant degree of geometrical complexity of the high-lift system. Also, the complexity of the geometry often leads to a large number of wake structures that all may individually impact the global flow. Despite a continuous improvement in CFD tools in the last decades, the accurate prediction of high-lift flows and the effect of geometrical details on the integrated forces and the stall behaviour still remains a challenge.

Over the course of several High-Lift Prediction Workshops[1] (HiLiftPW) it has by now been shown that current state-of-the-art CFD tools struggle to reliably predict the flow around high-lift configurations. During the HiLiftPW series, major focus was typically put on turbulence modelling and meshing as main sources for deviations between different solutions. However, this focus neglects other aspects that may fundamentally affect the ability to numerically predict high-lift flows. Some of those aspects, where the often-used steady-state RANS CFD tools introduce significant simplifications in the modelling, are in terms of time and geometry resolution, and in the modelling of wake structures. Firstly, time resolution is usually limited to forced steady-state solutions, due to the inherent increase in computational costs associated with unsteady simulations. Secondly, current grid generation technology often requires geometrical simplifications of the geometry to achieve sufficient mesh quality with acceptable turn-around times. And lastly, standard RANS tools employ numerical schemes that introduce high numerical dissipation that artificially dampens many flow structures.

Accurate prediction of the high-lift flow at and around maximum lift conditions therefore seems to require numerical methods that go beyond the current RANS methods. In this work, the Lattice Boltzmann Method (LBM) is considered as an alternative to state-of-the-art CFD tools, explicitly for the simulation of high-lift flows. LBM tools in general, and the method used here in particular, offer a number of advantages over classical CFD tools that address some crucial limitations. An example is given to highlight the effect of simulating with a reduced geometrical complexity, that is without taking slat and flap brackets into account. Then a short analysis of the unsteady behaviour of the high-lift flow around the stall condition is presented and the reasoning for time-accurate simulations discussed. Finally, a detailed comparison

of the capability to predict complex wake/vortex dominated flows is given and it is illustrated how RANS may deliver seemingly good results for the wrong reasons.

2 Computational Approach

The LBM code PowerFLOW is used for the simulation of the flow. PowerFLOW is a flow solver capable of addressing subsonic, transonic, and supersonic unsteady compressible flows based on extensions of the Lattice Boltzmann model.

2.1 Lattice Boltzmann Approach

LBM is a CFD technology developed over the last 30 years [2, 3] and has been validated for a wide variety of applications ranging from academic direct numerical simulation (DNS) cases [4] to industrial flow problems in the fields of aerodynamics [5, 6, 7, 8] and aeroacoustics [9, 10, 11]. Its motivation is to simulate a fluid at a microscopic level where the physics are simpler and more general [12] than the macroscopic continuum approach taken by the N-S equations. The latter can, however, be recovered from the LBM under certain conditions [13, 14, 15]. The unsteady nature of the LBM solution with low numerical dissipation makes the code especially well-suited for problems involving large-scale separated flows, as they occur on high-lift configurations around maximum lift conditions. The code offers a highly efficient local implementation of the LBM algorithm suitable for scalable distributed computations on thousands of processors.

2.2 Turbulence Modelling

The Lattice Boltzmann flow simulation is equivalent to a DNS of the flow. For high Reynolds number flows, such as those addressed in this work, the Lattice Boltzmann Very Large Eddy Simulation (LB-VLES) approach described in References [16, 17, 18] is used. It is conceptually similar to hybrid RANS/LES methods, like for example DES, where especially high Reynolds number boundary layers are modelled but large vortical structures are resolved with low dissipation [19]. This is expected to benefit the previously mentioned requirement to accurately capture wakes in the high-lift flow.

2.3 Wall Treatment

The Lattice Boltzmann bounce-back boundary condition for no-slip or the specular reflection for free-slip condition are generalized through a volumetric formulation [12, 20] near the wall for arbitrarily oriented surface elements (surfels) within the Cartesian volume elements (voxels). This formulation of the boundary condition on a curved surface cutting the Cartesian grid is automatically mass, momentum, and energy conservative while maintaining the spatial order of accuracy of the underlying LBM numerical scheme. To reduce the resolution requirements near the wall for high Reynolds number flows, a hybrid wall function is used to model the region of the boundary layer closest to a solid surface [21] including pressure gradients and compressibility effects.

2.4 Meshing Technique

Spatial discretisation in PowerFLOW is done using a Cartesian mesh approach. Local mesh refinement is done by successive factors of 2 in so-called Variable Refinement (VR) regions. Cartesian meshing not only supports the efficient implementation of the LBM scheme but it also enables fully automatic grid generation for arbitrarily complex geometries. This allows to avoid the mesh generation bottleneck of classical CFD tools, as it was highlighted by Slotnick et al. [22] and enables the detailed and accurate representation of high-lift configurations. An illustration of the Cartesian grid around a high-lift configuration is given in Figure 1.

3 Geometrical Complexity

When simulating high-lift configurations, every geometrical detail may matter and affect the global behaviour of the model. The typical goal for any high-lift configuration is to produce as much lift as possible with a given system layout.

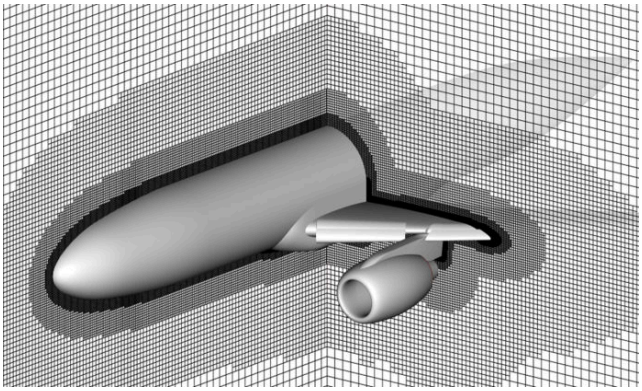

Fig. 1 : Illustration of the Cartesian grid around a high-lift model (coarsened for visualization)

For a desirable well-balanced wing design, this effectively means that not a single one of the highly loaded regions of the wing should stall at a significantly lower angle-of-attack than the rest of the wing. That is, the flow should approach separation simultaneously in several areas of the wing. And in those critical regions close to maximum lift, any small geometrical detail may alter the flow in a highly non-linear way.

This was reflected in the three AIAA High-Lift Prediction Workshops to date [1], where for the first workshop, the modelling of support brackets for slats and flaps was optional. For the second workshop, including the brackets was mandatory, but some additional small details (pressure tube bundles) were optional. It is interesting to note that one of those details actually triggered the wing stall in the wind tunnel measurements, as pointed out by Rudnik et al. [23]. For the third workshop, the bracket and fairing structures were again mandatory and were modelled even more accurately than before. Overall, the trend clearly shows that higher geometrical fidelity is considered important.

To illustrate the effect on the flow of simulating a simplified geometry, a surface streamline visualization for the JAXA High-Lift Standard Model (JSM) as it was used at the HiLiftPW-3 is shown in Figure 2. The original configuration in Figure 2b is compared to a simplified model with all brackets and fairing removed in Figure 2a. It is clearly visible at this angle-of-attack of $\alpha = 18.58°$ how the wakes of the slat tracks in particular lead to locally weakened flow and to an extended wing tip separation. Not including these geometrical details leads to a gross misprediction of the flow on the wing.

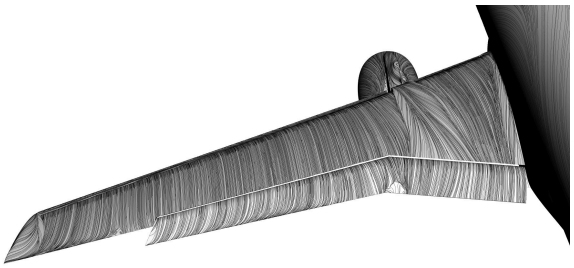

(a) Without slat and flap tracks

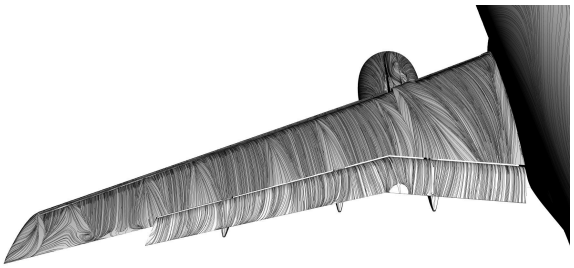

(b) Full configuration including tracks

Fig. 2 : Impact of the slat and flap brackets on the surface flow structures of the JSM Case 2 configuration.

The impact of the slat and flap brackets on the integrated forces is shown in Figure 3. As can be expected, the modelling of the brackets has a significant impact on the lift curve. Without the tracks, lift is consistently over-predicted by the simulation, leading to an over-prediction of $\Delta C_L = 0.15$ around $C_{L,max}$. But not only is lift over-predicted, the stall is also shifted towards a higher angle-of-attack. Hence, neglecting the brackets leads to an overall too optimistic assessment of the lift performance for this configuration. Similarly, the pitching moment is also altered when brackets are not included in the simulation and a more nose-down moment is predicted.

For this JSM configuration, the effect of neglecting the geometrical details of the brackets could probably be corrected for by means of an appropriate scaling and shifting as the fundamental stall behaviour is not altered. For the DLR-

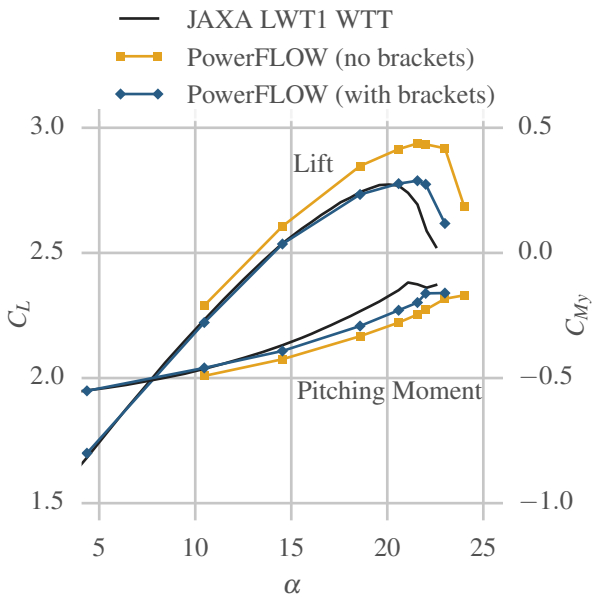

Fig. 3 : Impact of slat and flap brackets on the high-lift performance of the JSM Case 1.

F11 configuration, however, this is not true as was mentioned before and discussed by Rudnik et al. [23]. On that model, a little geometrical detail substantially altered the stalling mechanism. And without the capability to include this detail, no simulation could predict the characteristics properly. Obviously, for any new configuration it cannot be known a priori if any of the smaller geometrical details will have a significant impact or not. Being able to include all details in the simulations increases the likelihood of predicting the correct behaviour.

4 Time Accuracy

As a direct consequence of the large flow separations occurring around the stall condition, the flow is becoming more and more unsteady as the maximum lift is approached. To illustrate the degree of flow unsteadiness, two visualizations of the standard deviation of the surface pressure coefficient C_p for the JSM around $C_{L,max}$ are shown in Figure 4. Even before stall is reached, see Figure 4a, there are already significant fluctuations present in the flow, mostly in the wakes of the slat tracks, around the pylon, and at the wing tip. With the standard deviation of C_p reaching values of 0.5, the actual range of fluctuations is well in excess of $\Delta C_p = \pm 1$. Once the inboard wing has stalled, see Figure 4b, a large fraction of the lift-carrying part of the wing has turned unsteady with the fluctuation levels not being as high as around the slat tracks, but affecting a significantly larger area.

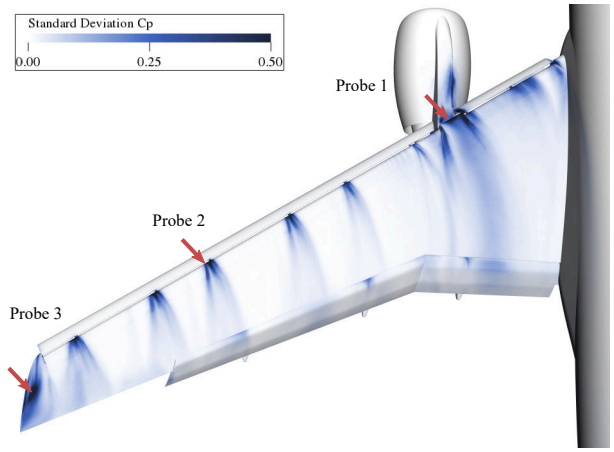

(a) $\alpha = 18.58°$

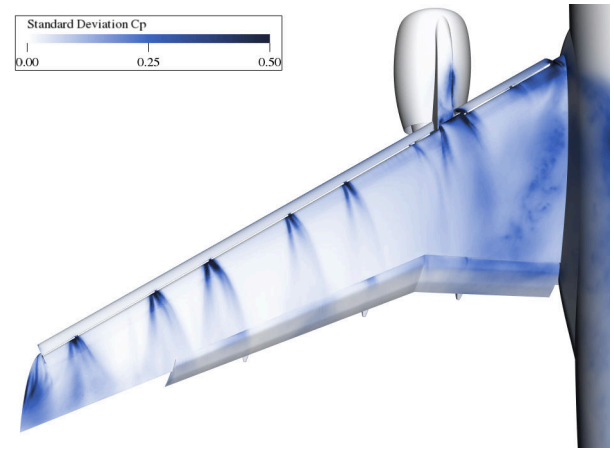

(b) $\alpha = 21.57°$

Fig. 4 : Illustrations of standard deviation of pressure on the JAXA JSM model around stall. Arrows mark locations of probes shown in Figure 5

For a more quantitative assessment, Figure 5 shows the power spectral density of the pressure fluctuations at three selected locations on the wing at an angle-of-attack of $\alpha = 18.58°$, corresponding to Figure 4a. The probe locations on the model's surface are also marked in Figure 4a. The three spectra all show elevated levels at frequencies of the order of around 1 kHz, indicating that a time-accurate solution of these phenomena requires small timesteps of the order of $t \lessapprox 10^{-4}$ s.

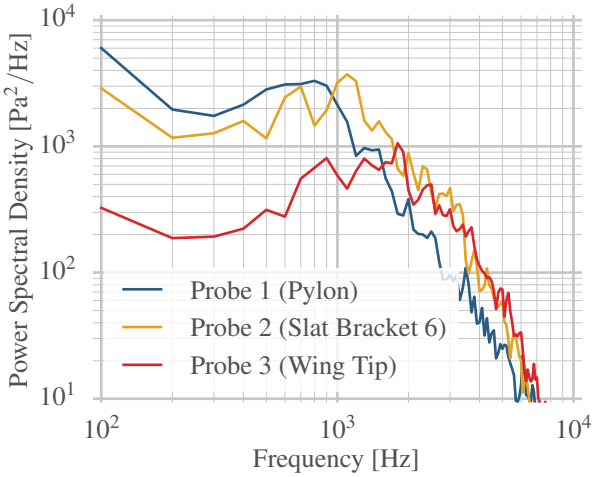

Fig. 5 : Power spectral density of pressure for selected probe locations.

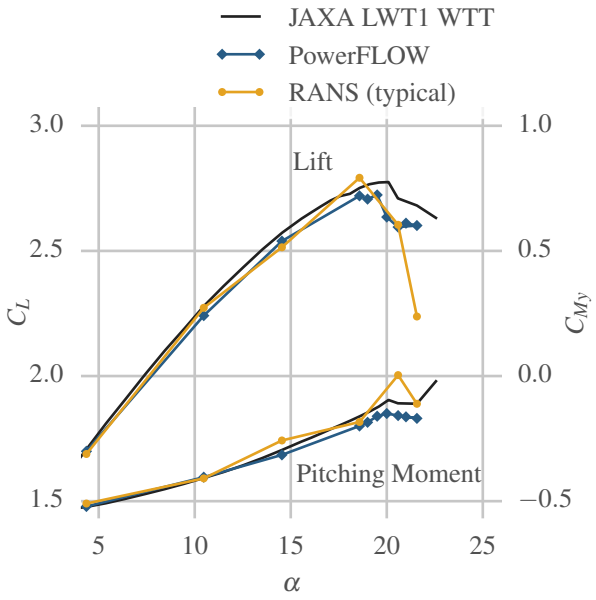

Fig. 6 : Lift and pitching moment comparison for the JSM Case 2. The RANS result is a representative solution from the HiLiftPW-3 (from [25] with permission)

A strong dependence of flow separation patterns of high-lift flows predicted by unsteady RANS solutions on the timestep was previously documented by Balin [24] for the DLR-F11 model. This shows that a time-accurate treatment can be crucial for the correct prediction of high-lift flows and that resolving the timescales properly is a demanding task.

5 Wake Modelling

In addition to the above mentioned differentiators between state-of-the-art RANS CFD and the current LBM tool, another noticeable difference became apparent at the HiLiftPW-3. Many of the RANS-based contributions to the workshop seemingly predicted the global lift behaviour well. But basically none of them were able to predict the correct local flow on the JSM in the wakes of slat brackets and the pylon.

Figure 6 shows lift and pitching moment for the JSM Case 2 configuration and compares a PowerFLOW result to a typical RANS solution. Both the RANS and PowerFLOW solutions are based on fully-turbulent simulations in free-air conditions, i. e. they did not take transition or installation effects into account which would play a noticeable role on this model. The RANS result was presented to HiLiftPW-3 by JAXA [25] using the Tohoku University Aerodynamic Simulation (TAS) code. It is representative for many other RANS results presented at the workshop that exhibited similar behaviour. Both simulation results show some deviation from the experimental results, with PowerFLOW slightly under-predicting $C_{L,max}$, and the RANS solution over-predicting it by a similar amount. From this integrated lift curve alone, both numerical methods seem to yield a comparable accuracy.

However, a detailed flow analysis reveals that the RANS result is giving an apparently good prediction of $C_{L,max}$ for the wrong reasons. To illustrate this, a surface flow visualization at stall condition ($\alpha = 21.57°$) of this typical RANS result is compared in Figure 7c to an oil flow image from the wind tunnel and to a PowerFLOW result. These images show the flow structures (wakes, vortices, and separations) that dominate the flow locally.

The oil flow image in Figure 7a is showing two large areas of separated flow, namely at the wing tip and at the wing root, with the latter being the major source of the lift-breakdown. Some weakening of the flow in the wake of the pylon and of the slat brackets on the mid-board wing

(a) JAXA LWT-1 (b) PowerFLOW (c) RANS

Fig. 7 : Visualization of flow separation patterns as seen in the wind tunnel, from PowerFLOW, and from a typical RANS method. The RANS result is a representative solution from the HiLiftPW-3 (from [25] with permission)

can also be seen but the flow still remains attached in those regions. The PowerFLOW result in Figure 7b shows a very good correlation of these flow structures to the experiment. Extent and shape of both the separations at the wing root and tip are accurately reproduced and even a small trailing edge separation outboard of the flap is capture correctly.

The RANS result in Figure 7c on the other hand shows a typical behaviour for many RANS tools in that it over-predicts the weakening of the flow in the wakes of pylon and slat brackets, leading to massive pre-mature separations, while at the same time under-predicting the corner separation at the wing root. Also, while there is a separation predicted at the wing tip, its structure seems different from the pattern seen in the wind tunnel. It can be generally stated that many of the RANS results presented to the HiLiftPW-3 showed similar trends. From this it seems clear that current RANS methods may have some deficiencies in modelling such wake flows correctly. It is interesting to note that the major areas of premature separation seen in this RANS result correlate to the areas with the highest unsteadiness found in Figure 4. At the same time, however, the side-of-body separation is located in a region with only moderate fluctuation levels, according to Figure 4.

In contrast to the difficulties common RANS methods seem to have with accurately prediction the numerous wake flows on high-lift configurations, the LBM method employed here is achieving a very good agreement to the experimental results on the JSM. Here, the proven lower dissipation capability of LBM versus standard RANS [26] together with the hybrid turbulence modelling approach employed in the current method enable a very accurate reproduction of all wake and separation features, especially the large separations at the wing root and tip.

In Figure 8 comparisons of the flow structures on the inboard wing and around the pylon are shown for two angles-of-attack at pre- and post-stall conditions. These detailed views illustrate that not only are the flow structures captured accurately at pre-stall condition, with still mostly attached flow. Also the progression to the large-scale separation at stall is correctly reproduced. Besides the good correlation of the flow structures on the wing surface, there is also a good agreement of the complex system of vortices and separations present on the nacelle and pylon. Hence, the good agreement of the integrated forces in Figure 6 is a result of consistently reproducing the correct flow physics.

It is particularly interesting to realize that the good correlation to the experiments in capturing the separation behaviour shown here was achieved by using a computational method that relies on wall functions to model the inner part of boundary layers. This contradicts the prevailing assumption that full resolution of boundary layers is required for accurate prediction of separations.

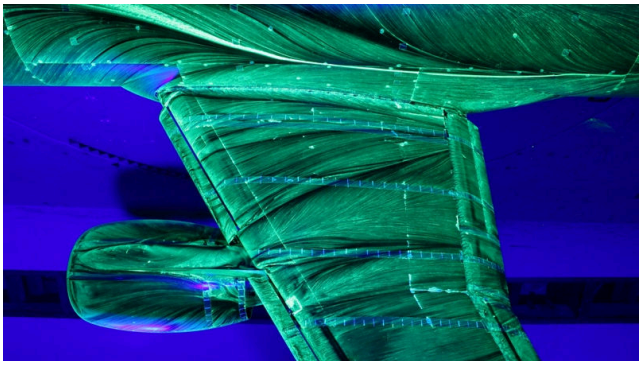

(a) Oil-flow, $\alpha = 18.58°$

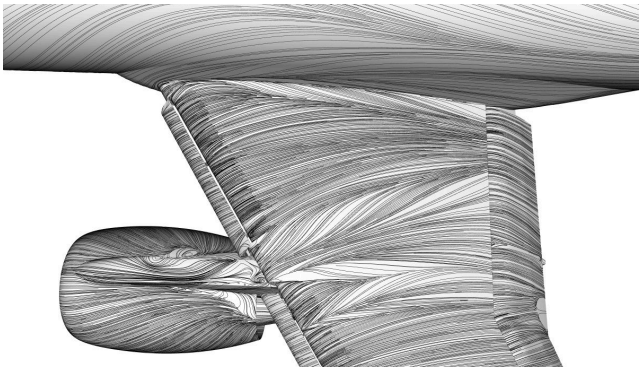

(b) Surface Streamlines PowerFLOW, $\alpha = 18.58°$

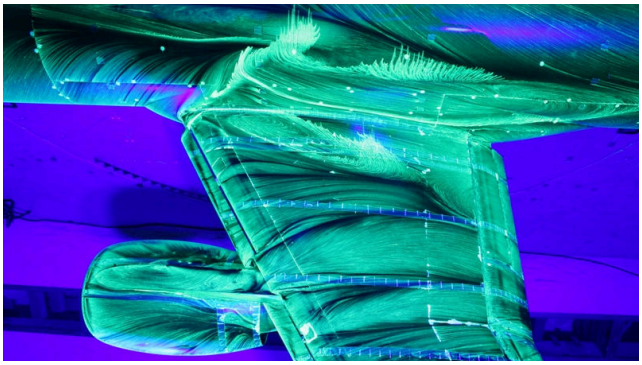

(c) Oil-flow, $\alpha = 21.57°$

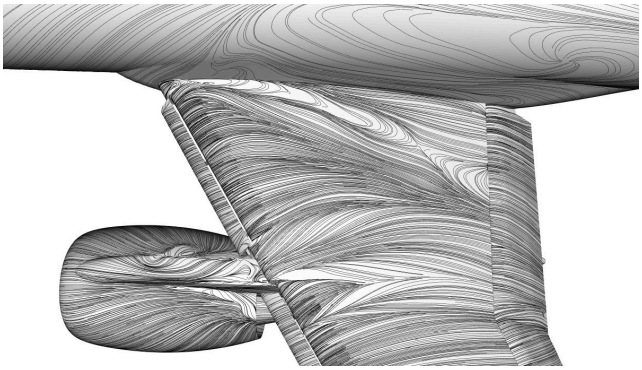

(d) Surface Streamlines PowerFLOW, $\alpha = 21.57°$

Fig. 8 : Surface flow visualizations of the wing root of the JSM Case 2 at pre- and post-stall conditions.

6 Conclusion

It is currently not yet fully understood what the limitations are that hinder the standard RANS methods to predict high-lift flows correctly. The focus of the High-Lift Prediction Workshop series so far was clearly on the impact of the turbulence modelling. However, the previous sections have shown that other factors may play a role as well.

It was demonstrated that the Lattice Boltzmann method used in this work is able to easily avoid some of the limitations that affect the current state-of-the-art tools used for high-lift predictions. Especially the very complex flows around high-lift configurations profit from the capabilities provided by Lattice Boltzmann based methods, namely the handling of arbitrarily complex geometries, the efficient time accurate modelling, and the low dissipation of wakes and vortices. It is also expected that the particular hybrid turbulence modelling approach of the PowerFLOW tool used in this work helps to accurately capture the complex flow phenomena of the various wake and vortex interactions.

In summary it has become clear from the previous High-Lift Prediction Workshop that the classical CFD methods struggle to accurately predict high-lift flows, especially around the maximum lift condition when the flow is dominated by large turbulent separations. Here the novel Lattice Boltzmann method offers a viable alternative that enables aerodynamics engineers to extend the range of application of CFD in the design and analysis of high-lift systems beyond what was previously feasible.

Copyright Statement

References

[1] AIAA CFD high lift prediction workshop series. http://hiliftpw.larc.nasa.gov/. Retrived April 2016.

[2] Chen H, Teixeira C and Molvig K. Digital physics approach to computational fluid dynamics: Some basic theoretical features. *International Journal of Modern Physics C*, Vol. 8, pp 675–684, 1997.

[3] Chen S and Doolen G D. Lattice boltzmann method for fluid flows. *Annual Review of Fluid Mechanics*, Vol. 30, pp 329–364, 1998.

[4] Ribeiro A F P, Casalino D, Fares E and Choudhari M. Direct numerical simulation of an airfoil with sand grain roughness on the leading edge. Tech. Rep, NASA Langley Research Center, NASA/TM-2016-219363, 2016.

[5] Khorrami M, Mineck R, Yao C and Jenkins N. A comparative study of simulated and measured gear-flap flow interaction. In *21st AIAA/CEAS Aeroacoustics Conference*, AIAA 2015-2989, 2015.

[6] König B *et al.* Lattice-boltzmann simulations of the JAXA JSM high-lift configuration. In *34th AIAA Applied Aerodynamics Conference*, AIAA 2016-3721, 2016.

[7] König B, Ribeiro A F and Fares E. Exa powerflow simulations for the sixth AIAA drag prediction workshop. In *55th AIAA Aerospace Sciences Meeting*, AIAA 2017-0963, 2017.

[8] Singh D, Ribeiro A F, König B and Fares E. Lattice boltzmann simulations of a supersonic cavity. In *35th AIAA Applied Aerodynamics Conference*, AIAA 2017-4461, 2017.

[9] Fares E, Duda B and Khorrami M R. Airframe noise prediction of a full aircraft in model and full scale using a lattice boltzmann approach. In *22nd AIAA/CEAS Aeroacoustics Conference*, AIAA 2016-2707, 2016.

[10] Casalino D *et al.* Towards lattice-boltzmann prediction of turbofan engine noise. In *20th AIAA/CEAS Aeroacoustics Conference*, AIAA 2014-3101, 2014.

[11] König B, Fares E, Ravetta P and Khorrami M R. A comparative study of simulated and measured main landing gear noise for large civil transports. In *23rd AIAA/CEAS Aeroacoustics Conference*, AIAA 2017-3013, 2017.

[12] Chen H. Volumetric formulation of the lattice boltzmann method for fluid dynamics: Basic concept. *Physical Review E* Vol. 58, pp 3955–3963, 1998.

[13] Chen H, Chen S and Matthaeus, W. H. Recovery of the navier-stokes equations using a lattice-gas boltzmann method. *Physical Review A*, Vol. 45, pp R5339–R5342, 1992.

[14] Qian Y, d'Humieres D and Lallemand P. Lattice BGK models for the navier-stokes equation. *Europhysics Letters*, Vol. 17, pp 479–484, 1992.

[15] Shan X, Yuan X-F and Chen H. Kinetic theory representation of hydrodynamics: a way beyond the navier stokes equation. *Journal of Fluid Mechanics*, Vol. 550, pp 413–441, 2006.

[16] Yakhot V and Orszag S A. Renormalization group analysis of turbulence. i. basic theory. *Journal of Scientific Computing*, Vol. 1, pp 3–51, 1986.

[17] Chen H *et al.* Extended boltzmann kinetic equation for turbulent flows. *Science*, Vol. 301, pp 633–636, 2003.

[18] Teixeira C M. Incorporating turbulence models into the lattice-boltzmann method. *International Journal of Modern Physics C*, Vol. 09, pp 1159–1175, 1998.

[19] Alexander C, Chen H, Kandasamy S, Shock R and Govindappa S. Simulations of engineering thermal turbulent flows using a lattice boltzmann based algorithm. In *ASME PVP, Proceedings of the 3rd International Symposium on Computational Technologies for fluid/thermal/chemical/stress systems with industrial applications*, 2001.

[20] Chen H, Teixeira C and Molvig K. Realization of fluid boundary conditions via discrete boltzmann dynamics. *International Journal of Modern Physics C*, Vol. 09, pp 1281–1292, 1998.

[21] Anagnost A *et al.* Digital physics analysis of the morel body in ground proximity. In *SAE International Congress and Exposition*, 1997. SAE

Technical Paper 970139.

[22] Slotnick J *et al.* CFD vision 2030 study: A path to revolutionary computational aerosciences. Tech. Rep, NASA Langley Research Center, NASA/CR-2014-218178, 2014.

[23] Rudnik R, Huber K and Melber-Wilkending S. Eurolift test case description for the 2nd high lift prediction workshop. In *30th AIAA Applied Aerodynamics Conference*, AIAA 2012-2924, 2012.

[24] Balin R. *The Effects of Time Step on Reynolds Averaged Navier-Stokes Simulations of High-Lift Flows*. Master's thesis, University of Colorado, 2016.

[25] Ito Y, Murayama M and Yamamoto K. TAS code results for the third high lift prediction workshop. In *Third AIAA High-Lift Prediction Workshop*, Japan Aerospace Exploration Agency (JAXA), 2017. URL `https://hiliftpw.larc.nasa.gov/Workshop3/HiLiftPW3-Presentations/011.pdf`.

[26] Marie S, Ricot D and Sagaut P. Comparison between lattice boltzmann method and navier-stokes high order schemes for computational aeroacoustics. *Journal of Computational Physics*, Vol. 228, pp 1056–1070, 2009.